Accurate electronic properties for (Hg,Cd)Te systems using hybrid density functional theory

Jeremy W. Nicklas and John W. Wilkins

Phys. Rev. B **84**, 121308 — Published 27 September 2011

DOI: 10.1103/PhysRevB.84.121308

Accurate electronic properties for HgCdTe systems using hybrid density functional theory

Jeremy W. Nicklas[1,*] and John W. Wilkins[1]

[1] *Department of Physics, The Ohio State University, Columbus, Ohio 43210, USA*

Hybrid screened density functional theory better describes the electronic structure of HgTe, CdTe, and HgCdTe systems in comparison with standard density functional theory. The newer hybrid functional reproduces the band inversion in the popular HgCdTe alloy justifying it as a better method than standard density functional theory in the search for new topological insulators. In addition, the 0.53 eV valence band offset obtained using the hybrid functional supports the recently observed higher band offset in the HgTe/CdTe heterostructure.

PACS numbers: 71.20.Nr, 71.23.-k, 71.55.Gs, 71.70.Ej, 73.20.At

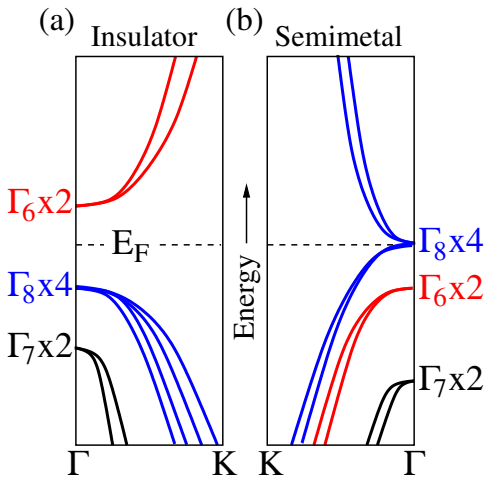

FIG. 1. (Color online) Schematic diagram of the bandstructure near the Γ point for (a) a cubic trivial bandgap insulator and (b) a semimetal. The bands below the Fermi level (dashed line) are filled and the ones above are empty.For a semimetal the s-like Γ_6 states lie below the Fermi level and are filled, whereas the p-like Γ_8 bands now form the top of the valence and bottom of the conduction band.

I. INTRODUCTION

The $Hg_{1-x}Cd_xTe$ alloy has a narrow gap range extending up to nearly the entire infrared spectrum. It is the material of choice for many high performance infrared detection applications. Recently it has come back under the spotlight for HgTe's topological insulating behaviour. A topological insulator has an insulating energy gap in the bulk states but conducting metallic states on the edges or surface. The 2D topological insulator exhibits a quantum spin Hall effect which was recently observed experimentally in HgTe/(Hg,Cd)Te quantum wells.[1,2] This has sparked an interest in finding new topological insulators by computing and finding band inversions in the band structure using standard density functional theory (DFT).[3,4] A more accurate treatment of the band structure can be achieved using a newer hybrid functional possibly improving upon the search for such materials, as shown for multinary chalcogenides.[5]

The Heyd-Scuseria-Ernzerhof (HSE) hybrid functional,[6,7] which combines the screened exchange with the Perdew-Burke-Ernzerhof (PBE) GGA functional,[8] has been seen to reproduce experimental electronic properties as well as band offsets for a range of III-V alloys.[9,10] This study extends upon those by reporting that HSE outperforms standard DFT on the electronic structure of the II-VI alloy $Hg_{1-x}Cd_xTe$ by reproducing the experimental crossover at $x = 0.17$ (Ref.[11]) transitioning from a semimetallic alloy with band inversion to a gapped semiconducting alloy. HSE also achieves a valence band offset (VBO) of 0.53 eV for HgTe/CdTe(001) agreeing with the more recent experimental data and settling a controversy on the VBO.[12,13]

Figure 1(a) describes a typical cubic trivial bandgap insulator (e.g., CdTe) with spin-orbit splitting. The conduction states exhibit s-like orbital symmetry and the Γ point possesses Γ_6 (twofold-degenerate) symmetry. The top of the valence band exhibits p-like orbital symmetry with a total angular momentum of $J = 3/2$ and a Γ point with Γ_8 (fourfold-degenerate) symmetry. The split-off band below that has a total angular momentum of $J = 1/2$ with a Γ point possessing Γ_7 (twofold-degenerate) symmetry. Figure 1(b) describes a semimetal (e.g., HgTe) where now the Γ_6 bands lie below the Γ_8 bands and are fully occupied, this is referred to as band inversion. By applying a lattice distortion to the semimetal the degeneracy in the Γ_8 states is lifted leading to a non-trivial bandgap, and hence a topological insulator.

II. METHOD

The calculations are performed using the projector augmented-wave (PAW) method.[14] The functionals included are the PBE[8] and the HSE06[7] hybrid functional in the VASP code.[15,16] The wavefunctions are expanded in plane waves up to an energy cutoff of 350 eV. The Brillouin-zone integration is carried out on an 8×8×8 Γ-centered k mesh over the full Brillouin-zone for the face-centered cubic primitive cell. Integrations over 4×3×3, 3×3×3, and 8×8×1 Γ-centered k meshes are used for the $x = 0.25$ and $x = 0.50$ special quasirandom stucture (SQS) supercells and the $4 + 4$ layer (001) heterostructure supercell, respectively.

The alloys are modeled by special quasirandom structures (SQSs),[17] ordered structures designed to reproduce the

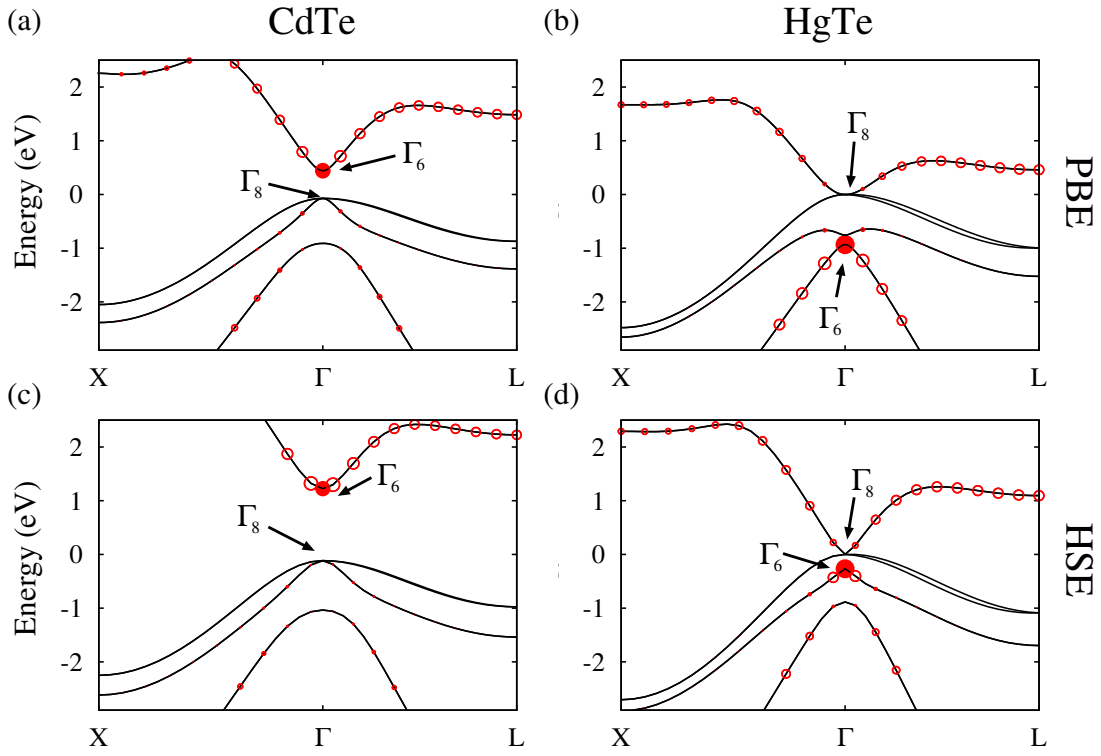

FIG. 2. (Color online) Projected bandstructure plots of the s-like state for (a) CdTe and (b)HgTe using PBE, as well as (c) CdTe and (d) HgTe using HSE. The size of the circles correspond to the weight of the s-like projection. The filled circle corresponds to the s-like projection at the Γ point, Γ_6. Arrows and proper labels point to the Γ_6 and Γ_8 locations in the bandstructures. HSE accurately reproduces the bandgap energy ($E_g = E_{\Gamma_6} - E_{\Gamma_8}$) for both CdTe and HgTe.

most important pair-correlation functions of a random alloy. We use our previously published 32-atom SQSs with Cd concentrations of 25%, 50%, and 75% for this alloy calculation.[9] The 25% and 75% SQSs, differing only by swapping Hg atoms with Cd atoms, match the pair-correlation functions of a random alloy up to 3rd nearest neighbor and the 50% SQS matches up to 7th nearest neighbor. The lattice constants for the $Hg_{1-x}Cd_xTe$ alloy are linearly interpolated between the experimental parent compound lattice constants of HgTe ($a = 6.46$ Å) and CdTe ($a = 6.48$ Å).[18] Relaxation is not taken into account due to the small lattice mismatch.

The heterostructure is described by a 4+4 layer thick supercell of 16 atoms with a (001) interface. An average of the experimental lattice constants of HgTe and CdTe is chosen as the lattice constant of the heterostructure. We employ the average electrostatic potential technique[19] to compute the valence band offset (VBO) of the heterostructure as

$$\mathrm{VBO} = \Delta E_{\mathrm{VBM}}^{(\mathrm{HgTe\text{-}CdTe})} - \Delta V_{\mathrm{step}}^{(\mathrm{HgTe\text{-}CdTe})} \tag{1}$$

where ΔE_{VBM} is the difference in the valence band maximas of the bulk HgTe and bulk CdTe and ΔV_{step} is the discontinuity in the reference potential across the heterostructure interface.

III. RESULTS

Figure 2 shows the projected bandstructure for both CdTe and HgTe obtained using the PBE and HSE functional with the top of the valence band set at 0 eV. The s-like projections are denoted by red circles with the weight of the projection being symbolized by the size of the circle. The Γ_6 projection is given by the solid red circle. Going from PBE to HSE the Γ_6 band is pushed upwards in both materials to at or near the correct experimental values. In the case of HgTe it reproduces the correct ordering of the Γ_8, Γ_6, and Γ_7 bands, respectively, whereas PBE reverses the ordering of the Γ_6 and Γ_7.

Table I compares the calculated bandgaps and spin-orbit splittings for both CdTe and HgTe against experiment. For discussion, the bandgap is taken as the energy difference between Γ_6 and Γ_8. For the case of a semimetal the bandgap will be "negative". The HSE functional yields bandgaps and splitting energies closer in magnitude to experiment than

TABLE I. The bandgap energy ($E_g = E_{\Gamma_6} - E_{\Gamma_8}$) and spin-orbit splitting energy ($\Delta_0 = E_{\Gamma_8} - E_{\Gamma_7}$) in units of eV for both CdTe and HgTe computed using both HSE and PBE compared with experiment. Note that although HSE tends to underestimate CdTe bandgap by 16%, PBE in stark contrast underestimates it by 68%.

	HSE	PBE	Exp
CdTe			
E_g	1.34	0.52	1.6[a]
Δ_0	0.92	0.84	0.95[b]
HgTe			
E_g	-0.27	-0.93	-0.29[c]
Δ_0	0.89	0.76	0.91[c]

[a] From Ref.[20].
[b] From Ref.[21].
[c] From Ref.[22].

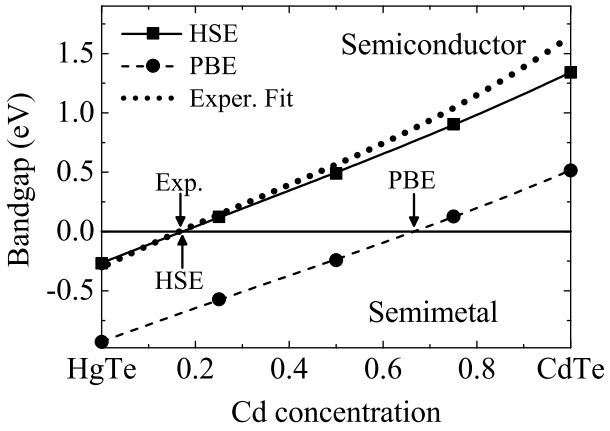

FIG. 3. Bandgap (defined as $E_{\Gamma_6} - E_{\Gamma_8}$) versus alloy concentration of $Hg_{1-x}Cd_xTe$ computed using HSE (solid line) and PBE (dashed line) compared to experiment (dotted line).[11] A positive bandgap corresponds to a trivial gap semiconductor and a negative bandgap corresponds to a semimetal. The data points used for the fits are shown as squares and circles for HSE and PBE, respectively. The crossovers from semimetal to semiconductor for each functional and experiment are labeled by arrows. HSE agrees with experiment for not only the bandgap magnitude but also the alloy's transition from a semimetal to a normal gap semiconductor.

PBE for both materials. Even though HSE was initially developed to compute accurate bandgaps for semiconductors in mind, it still manages to reproduce the negative bandgap value for HgTe.

The bandgap ($\Gamma_6 - \Gamma_8$ energy difference) versus Cd concentration for the $Hg_{1-x}Cd_xTe$ alloy is plotted in Figure 3. A cubic fit is used for the five data points taken at the end points and Cd concentrations of 25%, 50%, and 75% for the calculated values. The HSE fit lies nearly on top of the experimental fit[11] for smaller concentrations of Cd while slightly underestimating the magnitude at higher concentrations. PBE grossly underestimates this bandgap while failing to predict it as a semiconducting alloy throughout much of the alloy range.

Table II lists the computed Cd compositions at which the $Hg_{1-x}Cd_xTe$ alloy goes from semimetallic to a trivial bandgap semiconductor. HSE reproduces the experimental crossover to two significant figures. The ability to predict band inversion across an entire alloy has major implications in the search for new topological insulators. Standard density functional theory such as PBE tends to underestimate the bandgap as seen here, this can lead to the prediction of false-positives when looking for topological insulators.

The valence band offset (VBO) is calculated for the HgTe/CdTe(001) interface using HSE. The HSE functional yields a VBO of 0.53 eV in contrast to previous self-consistent calculations of 0.27 eV,[24] 0.22 eV,[25] and 0.37 eV.[26] HSE is in excellent agreement with the more recent experimental values of 0.53±0.06 eV[12] and 0.55±0.05 eV[13] in contradiction with earlier x-ray and ultraviolet photoelectron spectroscopy which provide a VBO around 0.35 eV.[27–29] Eich *et al.*[12] demonstrate that an accurate treatment of the band dispersion in HgTe at the valence band edge is necessary for a correct measurement of the VBO leading to the higher observed VBO. HSE in this case lends strong support for this higher band offset.

TABLE II. The Cd concentration in $Hg_{1-x}Cd_xTe$ at which the alloy goes from being semimetallic to a trivial bandgap semiconductor labeled by $x_{\text{crossover}}$. HSE yields a crossover composition in very good agreement with experiment. PBE predicts the alloy to be semimetallic throughout most of the composition.

	HSE	PBE	Exp
$x_{\text{crossover}}$	0.17	0.67	0.17[a], 0.16[b]

[a] Using the fit from Ref.[11].
[b] Using the fit from Ref.[23].

IV. CONCLUSIONS

We present a hybrid functional study of the electronic properties of HgTe and CdTe. The calculated bandstructures using HSE show better bandgaps and band ordering compared with experiment than standard DFT for bulk HgTe and CdTe. Our results confirm that (a) HSE is superior in reproducing the semimetal to semiconductor transition in the $Hg_{1-x}Cd_xTe$ alloy providing a solid basis for future work in topological insulator studies, and (b) HSE strengthens the argument for a higher VBO of 0.53 eV in the HgTe/CdTe interface.

V. ACKNOWLEDGMENTS

This work was supported by DOE-Basic Energy Sciences, Division of Materials Sciences (Grant No. DE-FG02-99ER45795). Computational resources were provided in part by an allocation of computing time from the Ohio Supercomputer Center and the National Energy Research Science Computing Center. The latter is supported by the Office of Science of the U.S. Department of Energy under Contract No. DE-AC02-05CH11231. We are also grateful to Amita Wadehra for her useful comments.

* nicklas.2@buckeyemail.osu.edu

[1] M. König, S. Wiedmann, C. Brüne, A. Roth, H. Buhmann, L. W. Molenkamp, X.-L. Qi, and S.-C. Zhang, Science **318**, 766 (2007).
[2] A. Roth, C. Brüne, H. Buhmann, L. W. Molenkamp, J. Maciejko, X.-L. Qi, and S.-C. Zhang, Science **325**, 294 (2009).
[3] S. Chadov, X. Qi, J. Kübler, G. H. Fecher, C. Felser, and S. C. Zhang, Nature Mat. **9**, 541 (2010).
[4] H. Lin, L. A. Wray, Y. Xia, S. Xu, S. Jia, R. J. Cava, A. Bansil, and M. Z. Hasan, Nature Mat. **9**, 546 (2010).
[5] S. Chen, X. G. Gong, C.-G. Duan, Z.-Q. Zhu, J.-H. Chu, A. Walsh, Y.-G. Yao, J. Ma, and S.-H. Wei, Phys. Rev. B **83**, 245202 (2011).
[6] J. Heyd, G. E. Scuseria, and M. Ernzerhof, J. Chem. Phys. **118**, 8207 (2003).
[7] J. Heyd, G. E. Scuseria, and M. Ernzerhof, J. Chem. Phys. **124**, 219906 (2006).
[8] J. P. Perdew, K. Burke, and M. Ernzerhof, Phys. Rev. Lett. **77**, 3865 (1996).
[9] J. W. Nicklas and J. W. Wilkins, Appl. Phys. Lett. **97**, 091902 (2010).
[10] A. Wadehra, J. W. Nicklas, and J. W. Wilkins, Appl. Phys. Lett. **97**, 092119 (2010).
[11] G. L. Hansen, J. L. Schmit, and T. N. Casselman, J. Appl. Phys. **53**, 7099 (1982).
[12] D. Eich, K. Ortner, U. Groh, Z. H. Chen, C. R. Becker, G. Landwehr, R. Fink, and E. Umbach, Phys. Stat. Sol. (a) **173**, 261 (1999).
[13] Z. Yang, Z. Yu, Y. Lansari, S. Hwang, J. W. Cook, and J. F. Schetzina, Phys. Rev. B **49**, 8096 (1994).
[14] P. E. Blöchl, Phys. Rev. B **50**, 17953 (1994).
[15] G. Kresse and J. Furthmuller, Phys. Rev. B **54**, 11169 (1996).
[16] G. Kresse and D. Joubert, Phys. Rev. B **59**, 1758 (1999).
[17] S.-H. Wei, L. G. Ferreira, J. E. Bernard, and A. Zunger, Phys. Rev. B **42**, 9622 (1990).
[18] T. Skauli and T. Colin, J. of Crys. Growth **222**, 719 (2000).
[19] A. Baldereschi, S. Baroni, and R. Resta, Phys. Rev. Lett. **61**, 734 (1988).
[20] Landolt-Börnstein, *Semiconductors: Intrinsic properties of group IV elements and III-V, II-VI and I-VII compounds*, edited by O. Madelung, W. Van der Osten, and U. Rössler, Group III, Vol. 22 (Springer Verlag, Berlin, 1987) p. 210.
[21] A. Twarkdowski, E. Rokita, and J. A. Gaj, Solid State Comm. **36**, 927 (1980).
[22] N. E. Orlowski, J. Augustin, Z. Golacki, C. Janowitz, and R. Manzke, Phys. Rev. B **61**, R5058 (2000).
[23] J. Chu, S. Xu, and D. Tang, Appl. Phys. Lett. **43**, 1064 (1983).
[24] N. E. Christensen, Phys. Rev. B **38**, 12687 (1988).
[25] A. Qteish and R. J. Needs, Phys. Rev. B **47**, 3714 (1993).

[26] S.-H. Wei and A. Zunger, Phys. Rev. Lett. **59**, 144 (1987).
[27] S. P. Kowalczyk, J. T. Cheung, E. A. Kraut, and R. W. Grant, Phys. Rev. Lett. **56**, 1605 (1986).
[28] R. S. Sporken, S. Sivananthan, J. P. Faurie, D. H. Ehlers, J. Fraxedos, L. Ley, J. J. Pireaux, and R. Caudano, J. Vac. Sci. Technol. A **7**, 427 (1989).
[29] C. K. Shih and W. E. Spicer, Phys. Rev. Lett. **58**, 2594 (1987).